Drug Design, Development and Therapy

Dovepress
open access to scientific and medical research

Open Access Full Text Article

ORIGINAL RESEARCH

Integrated Network Pharmacology, Molecular Docking and Animal Experiment to Explore the Efficacy and Potential Mechanism of Baiyu Decoction Against Ulcerative Colitis by Enema

Yuan Cui[1,2], Jingyi Hu[2], Yanan Li[1,2], Ryan Au[1,2], Yulai Fang[2], Cheng Cheng[1], Feng Xu[1,2], Weiyang Li[1,2], Yuguang Wu[1,2], Lei Zhu[2], Hong Shen[2]

[1]Nanjing University of Chinese Medicine, Nanjing, People's Republic of China; [2]Affiliated Hospital of Nanjing University of Chinese Medicine, Nanjing, People's Republic of China

Correspondence: Lei Zhu; Hong Shen, Tel/Fax +86-25- 86617141, Email shenhong999@njucm.edu.cn; zhulei5100@njucm.edu.cn

Background: Baiyu Decoction (BYD), a clinical prescription of traditional Chinese medicine, has been proven to be valuable for treating ulcerative colitis (UC) by enema. However, the mechanism of BYD against UC remains unclear.

Purpose: A combination of bioinformatics methods including network pharmacology and molecular docking and animal experiments were utilized to investigate the potential mechanism of BYD in the treatment of UC.

Materials and Methods: Firstly, the representative compounds of each herb in BYD were detected by liquid chromatography-mass spectrometry. Subsequently, we predicted the core targets and potential pathways of BYD for treating UC through network pharmacology. And rat colitis model was established with dextran sodium sulfate. UC rats were subjected to BYD enema administration, during which we recorded body weight changes, disease activity index, and colon length to assess the effectiveness of BYD. Besides, quantitative real-time PCR, western blotting, ELISA and immunofluorescence were used to detect intestinal inflammatory factors, intestinal barrier biomarkers and TOLL-like receptor pathway in rats. Finally, the core components and targets of BYD were subjected to molecular docking so as to further validate the results of network pharmacology.

Results: A total of 41 active compositions and 203 targets related to BYD-UC were subjected to screening. The results of bioinformatics analysis showed that quercetin and kaempferol may be the main compounds. Additionally, AKT1, IL-6, TP53, TNF and IL-1β were regarded as potential therapeutic targets. KEGG results explained that TOLL-like receptor pathway might play a pivotal role in BYD protecting against UC. In addition, animal experiments and molecular docking validated the network pharmacology results. BYD enema treatment can reduce body weight loss, lower disease activity index score, reverse colon shortening, relieve intestinal inflammation, protect intestinal barrier, and inhibit TOLL-like receptor pathway in UC rats. Besides, molecular docking suggested that quercetin and kaempferol docked well with TLR4, AKT1, IL-6, TP53.

Conclusion: Utilizing network pharmacology, animal studies, and molecular docking, enema therapy with BYD was confirmed to have anti-UC efficacy by alleviating intestinal inflammation, protecting the intestinal barrier, and inhibiting the TOLL-like receptor pathway. Researchers should focus not only on oral medications but also on the rectal administration of medications in furtherance of the cure of ulcerative colitis.

Keywords: network pharmacology, ulcerative colitis, enema therapy, TLR4/MyD88/NF-κB pathway

Introduction

Ulcerative colitis (UC) is featured with mucosal inflammation that begins with rectum and spreads to the proximal colon.[1] The typical symptoms of UC include abdominal pain, acute or chronic diarrhea, and bloody stools. Pathogenesis of UC is still unclear, and an increasing number of studies suggest that it is mainly caused by immune dysregulation, intestinal epithelial barrier defects, intestinal microbial changes and environmental factors.[2] The popular therapeutic

Received: 9 September 2023
Accepted: 9 November 2023
Published: 23 November 2023

Graphical Abstract

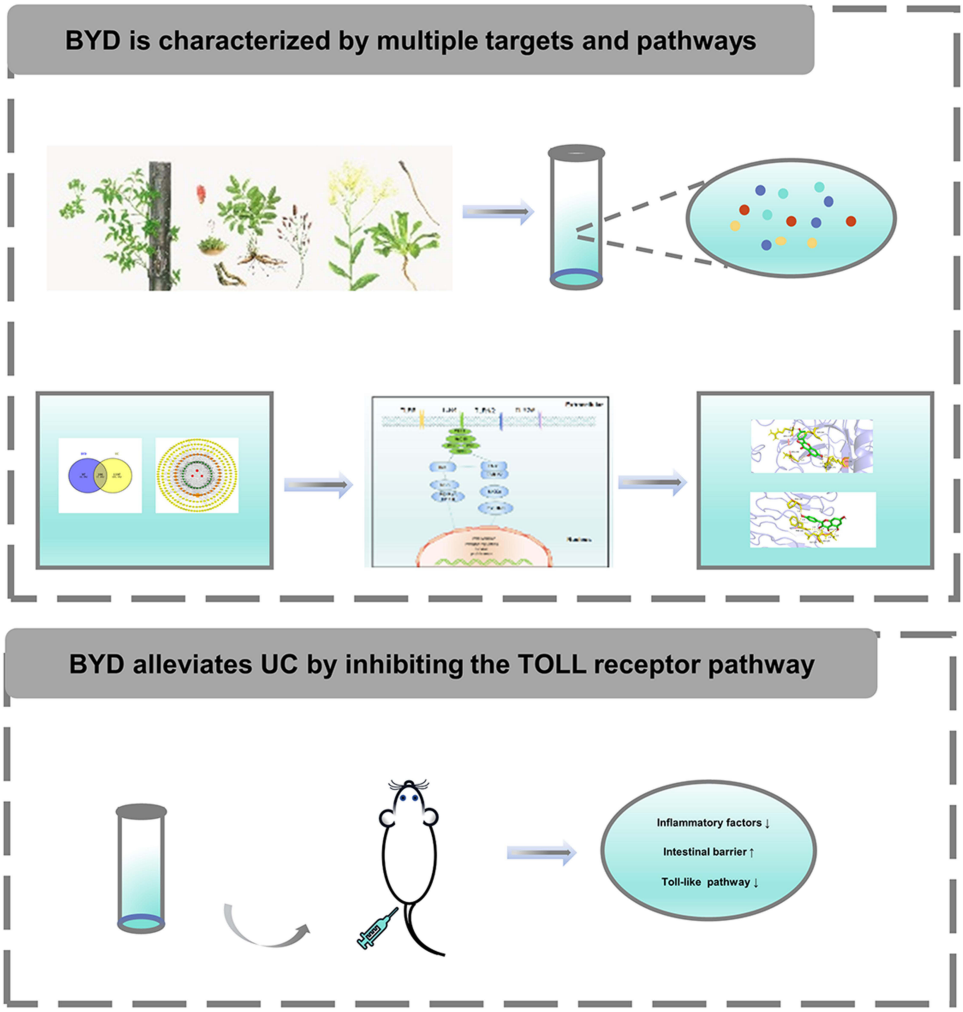

medicines for UC are 5-aminosalicylic acid (5-ASA), biological agents and immunosuppressants.[3] Although above drugs can relieve symptoms to some extent, in addition to being expensive, they can also cause many adverse effects,[4,5] which brings heavy economic burden and psychological pressure to UC patients.

Traditional Chinese medicine (TCM) with unparalleled theoretical system differs from modern medicine distinctly. Baiyu Decoction (BYD) is a prescription created by Professor Shen for the treatment of UC by enema, which can dramatically alleviate the clinical symptoms of most UC patients. BYD is composed of three Chinese herbs, *Phellodendron amurense* Rupr. (Chinese name Huangbai; HB), *Sanguisorba officinalis* L. (Chinese name Diyu; DY), *Indigofera suffruticosa* Mill. (Chinese name Qingdai; QD), which have been commonly used for UC in TCM since ancient time. The plant name has been verified with MPNS (http://mpns.kew.org). The multiple functions of BYD are clearing dampness and heat, cooling blood and removing blood stasis, and hemostasis.

Network pharmacology put forward by Andrew L. Hopkins specifies the process of diseases and emphasizes the analysis of the molecular association between drugs and therapeutic objects from the view of biological network.[6,7] The method of network pharmacology has been broadly employed in the innovation of Chinese herbs.[8] It provides new ideas for the study of complex system of TCM and scientific and technological support for clinical practice.[9] Molecular docking studies the interaction between different molecules and predicts their binding affinities and modes.[10,11]

The active ingredients and pharmacological effects of the three herbs of BYD, HB, DY and QD have been extensively studied. HB could clear heat, dry dampness, drain fire, eliminate steam, resolve toxin, and treat sores according to the theory of TCM. Modern pharmacological researches show the most important chemical constituents of HB are alkaloids containing berberine and jatrorrhizine.[12] HB has a variety of pharmacological effects, including immunomodulatory, anti-inflammatory, antibacterial, anticancer, hypotensive, antiarrhythmic, antioxidant, and antiulcer.[12] HB treatment increased the abundance of intestinal flora and beneficial bacteria and regulates the AMPK-mTOR signaling pathway to promote autophagy, thus reducing the damage of UC to the intestine.[13] The active components of DY are dominated by flavonoids, triterpenoids, phenolic compounds.[14] Many experiments have shown that DY involves anti-inflammatory, anti-cancer, anti-lipid peroxidation, anti-bacterial, anti-diabetic, hepatoprotective and anti-obesity effects.[14] DY and its active ingredients ameliorated DSS-induced colitis by inhibiting intestinal inflammation through promoting Atg7-dependent autophagy.[15] QD has been applied to detoxification, defervescence, detumescence and antiphlogosis. Glycosides and alkaloids have been obtained from QD, and the functions of QD encompass anti-cancer, inflammation relief, microbial inhibition, and skin disease relief.[16] In one placebo-controlled trial, Curcumin-QingDai was effective for inducing response and remission in active UC patients, and the aryl-hydrocarbon receptor pathway might be potential therapeutic target for UC.[17] QD could regulate intestinal flora, reduce inflammation, repair intestinal mucosa, and improve the physiological status of DSS-induced UC mice and its anti-UC mechanism may be involved in inhibiting TLR4/MyD88/NF-κB signal transduction.[18] Although the above studies proved the therapeutic effect of HB, DY and QD on UC, there is paucity of literature on the treatment of UC by enemas with all three herbs.

In this paper, firstly, we conducted a network pharmacology study on the ground of the main components of BYD and the component-target-disease interactions. Subsequently, an acute colitis model in rats was established to verify the network pharmacology results. Finally, molecular docking experiments were performed for further verification. The flow chart of the study is shown in Figure 1.

Materials and Methods

Collection of the Compounds of BYD and UC-Related Targets

All active compounds and protein targets of BYD were obtained from TCMSP (https://old.tcmsp-e.com/tcmsp.php),[19] according to the thresholdBPs of Drug-like (DL)≥0.18 and Oral bioavailability (OB)≥30%. Human gene name and gene ID were collected from the UniProt database (https://www.uniprot.org/).[20] Targets about "ulcerative colitis" were obtained from GeneCards (https://www.genecards.org/), OMIM (https://omim.org/),[21] TTD (http://db.idrblab.net/ttd/) and DrugBank (https://go.drugbank.com/). After removing duplicate gene, the overlapping data on target genes related to UC and active compounds were retained as candidate targets. The above data were inputted to the Cytoscape 3.9.1 for herb-compound-target network and Venny 2.1.0 (https://bioinfogp.cnb.csic.es/) for distribution of BYD potential targets and UC targets.

Protein–Protein Interaction (PPI) Network Analysis

The overlapping data on target genes related to UC and active compounds were imported into STRING 11.5 (https://cn.string-db.org/) for PPI analysis.[22] Homo sapiens is listed as restricted species. Then PPI results exported from STRING 11.5 were imported into Cytoscape 3.9.1 in order to get another more visual network diagram.

GO and KEGG Enrichment Analysis

The data, firstly, obtained from STRING 11.5 were processed and imported into Metascape (https://metascape.org/) for enrichment analysis. The GO data include cellular component (CC), biological process (BP) and molecular function (MF). Subsequently, every top 20 items in CC, BP, and MF and top 30 pathways in KEGG were selected to the Bioinformatics platform (http://www.bioinformatics.com.cn/) for visual analysis.[23]

Molecular Docking

According to the network pharmacology results, the top 2 components of BYD and the core protein targets were molecularly docked to judge the affinity of their interactions. The specific steps are as follows: (1) Acquisition of protein and component

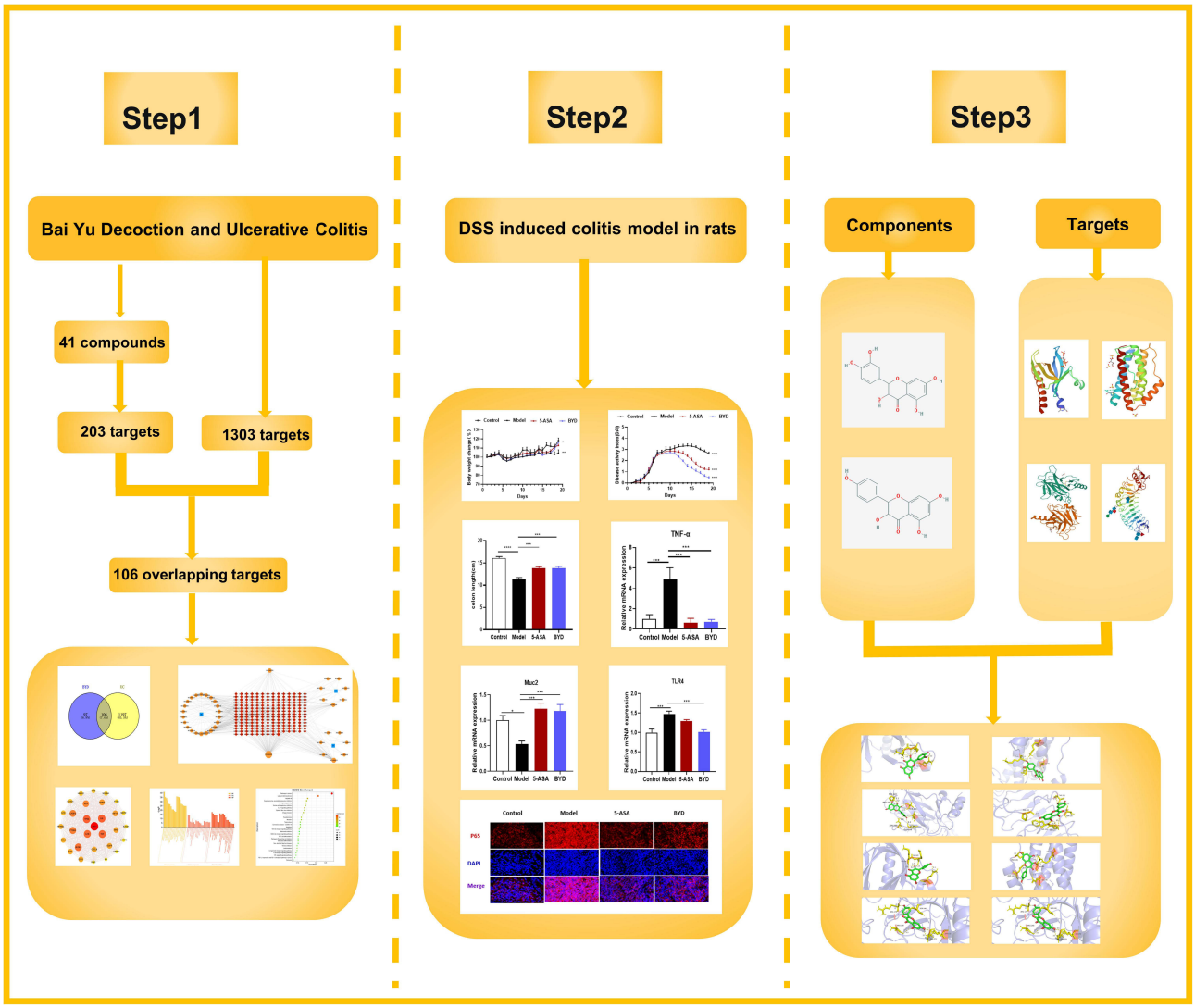

Figure 1 The framework of this study.

files: We obtained the MOL2 format files of compounds from the TCMSP database and downloaded the PDB format files of target proteins from the PDB Database (https://www.rcsb.org/). (2) Setting of the protein receptor: First, use PyMol software to remove the water and solvent of the protein. Then, use AutoDock4 to add hydrogen. Finally, set it as protein receptor and save it as a PDBQT format file. (3) Setting of the component ligand: Similarly, add hydrogen to the component in AutoDock4 software and set the component as ligand. Subsequently, the torsion tree was automatically configured in the software before exporting component ligand as PDBQT format files. (4) Molecular docking: After importing the PDBQT files of the protein receptor and component ligand into AutoDock4, the size of the docking box was adjusted to completely cover the active site of the protein receptor and the docking parameters were set for molecular docking. (5) Result description and visualization: the binding energy of molecular docking <0 kcal/mol indicates that the docking is in the natural state, and the binding energy < −1.2 kcal/mol suggests the docking result is ideal. Therefore, the results with the smallest binding energy are generally selected and imported into PyMol for visualization.

Preparation of BYD and LC-MS/MS Analysis

BYD, HB (18 g), DY (9 g) and QD (3 g) were bought from Jiangsu Province Hospital of Chinese Medicine. The proportions of HB, DY and QD are 60%, 30% and 10%, respectively. Three herbs were mixed and soaked for 30 minutes with 10 times (w/v)

distilled water, followed by boiling for 40 minutes twice. The two extracted solutions were mixed and further concentrated to 0.31 g/mL. Ultimately, the main compounds of BYD were detected by liquid chromatography-mass spectrometry (LC-MS /MS). 5 μL aliquots of prepared BYD were passed through a 0.22 μm filter into auto-sampler vials for analysis using ultra high-performance liquid chromatography (UHPLC)-electrospray ionization (ESI)-Q-orbitrap-mass spectrometry (MS) system, utilizing the Shimadzu Nexera X2 LC-30AD (Shimadzu, Japan) combined with the Q Exactive™ Plus Hybrid Quadrupole-Orbitrap™ Mass Spectrometer (Thermo Scientific, San Jose, USA). ACQUITY UPLC® high strength silica (HSS) T3 columns (2.1×100 mm, 1.8μm) (Waters, Milford, MA, USA) were used for liquid chromatography separation with a flow rate of 0.3 mL/min. The mobile phases were A: 0.1% formic acid in water and B: 100% acetonitrile. The elution gradient was as follows: 0% B for 2 minutes, linearly increased to 48% B in 4 minutes, and up to 100% B in 4 minutes and maintained for 2 minutes. Raw MS data were imported into MS-DIAL for further processing, including correction of retention times, alignment of peaks, and extraction of peak areas. BYD constituents were identified by matching peak information found in Shanghai BIOPROFILE Co, Ltd' s in-house secondary mass spectrometry database.

Reagents

Dextran sodium sulfate (DSS, M. W. = 36–50 kDa,160110) was obtained from MP Biomedicals (California, USA). Isoflurane (R510-22-8) was purchased from RWD (Shenzhen, China). 5-Aminosalicylic acid (5-ASA, A79809) was bought from Sigma-Aldrich (USA). cDNA Synthesis Kit (R211-01) and qRT-PCR SYBR Green Kit (Q221-01) were provided by Vazyme Biotech (Nanjing, Jiangsu, China). TNF-α (ZC-37624), IL-6 (ZC-36404), IL-10 (ZC-36379), IL-1β (ZC-36391) ELISA kits were purchased from ZCIBIO Technology (Shanghai, China). Bicinchoninic acid (BCA, P0010) protein assay kit, and phenylmethanesulfonyl fluoride (PMSF, P1005) were purchased from Beyotime (Shanghai, China). Anti-TLR4 (19811–1-AP), anti-MyD88 (23230–1-AP), β-actin (66009–1-Ig), HRP-conjugated Affinipure Goat-Anti-Mouse IgG (H+L) (SA00001–1) and HRP-conjugated Affinipure Goat-Anti-Rabbit IgG (H+L) (SA00001–2) were purchased from Proteintech Group (Rosemont, USA). Anti-ZO-1 (sc-33725) was purchased from Santa Cruz Biotechnology (USA). Anti-MUC2 (ab272692) was obtained from Abcam (Cambridgeshire, UK). NF-κB (#8242) and Phospho-NF-κB (#3033) were bought from Cell Signaling Technology (Danvers, MA, USA). Enhanced chemiluminescent (ECL, BL520B) plus reagent kit was purchased from Biosharp (Hefei, Anhui, China).

Animals and Treatment

Forty male Sprague Dawley rats (weighting 200 ± 20 g) were purchased from Shanghai Family Planning Research Institute (Shanghai, China). On arrival, all rats were kept in a specific-pathogen-free room under a 12-h light/dark cycle (Animal usage license number: SYXK (Su) 2022–0070). After adaptive feeding, rats were randomly divided into 4 groups: Control group, Model group, 5-ASA group, and BYD group. Each group contains ten rats. The animal studies were approved by the Animal Ethics Committee in Affiliated Hospital of Nanjing University of Traditional Chinese Medicine (Application Number: 2023DW-030-01) in accordance with the guidelines of the Guide for the Care and Use of Laboratory Animals.

According to previous literature description, acute colitis was induced by administration of 4% (w/v) DSS in drinking water for 7 days, in order to maintain colitis model, rats were then given 3% DSS for 7 days.[24] Except for the control group, the other 3 groups were treated by intrarectal administration for 12 consecutive days from the first day of drinking 3% DSS. Before enema therapy, the rats were fasted for 12 hours to empty rats' intestines. After rats were anesthetized with Isoflurane, the 16-gauge gavage needle with 2 mL solution was inserted into the rat's anus for 8 cm slowly and gently. Then the rats were inverted for 5 minutes to prevent drug outflow and finally returned to the cage and raised normally. During the experiment, the water and food intake, mental state and fur gloss of the rats were observed every day. And the disease activity index (DAI) was calculated as previously described (Table 1).[25] At the end of the experiment, rats were anaesthetized by Isoflurane, and blood was collected from the femoral artery. After spinal dislocation, the rats' colon was harvested and measured.

Table 1 Disease Activity Index

Stool Traits	Bloody Stool	Weight Loss (10%)	DAI Score
Normal	Negative of occult blood	None	0
Mild soft stool	Occult blood weakly positive (+)	1–5%	1
Severe soft stool	Occult blood positive (++)	5–10%	2
Mild diarrhea	Occult blood strongly positive (+++)	10–15%	3
Severe diarrhea	Bloody naked eye	>15%	4

H&E and AB-PAS Staining

1 cm colon tissue was fixed in paraformaldehyde and embedded in paraffin. Paraffin-embedded sections (4 μm) were stained with H&E and AB-PAS for evaluating colon morphology, mucus layer and goblet cells. Then, pathological scores were calculated (Table 2).[26]

Quantitative Real-Time PCR (qRT-PCR)

After RNA and cDNA extraction, SYBR Green Kit was utilized to quantify mRNA levels in accordance with manufacturer's protocols. GADPH was taken as internal control. Primer sequences are listed in Table 3.

Table 2 Pathological Scores

Feature	Grade	Description
Inflammation level	0	None
	1	Slight
	2	Moderate
	3	Severe
Inflammation extent	0	None
	1	Mucosa
	2	Mucosa and submucosa
	3	Transmural
Crypt damage	0	None
	1	Basal 1/3 damaged
	2	Basal 2/3 damaged
	3	Only surface epithelium intact
	4	Entire crypt and epithelium lost
Involvement Percentage	1	1–25%
	2	26–50%
	3	51–75%
	4	76–100%

Table 3 Primer Sequences

Gene		Primers
IL-1β	F	GCAGCTTTCGACAGTGAGGA
	R	CCCAAGTCAAGGGCTTGGAA
TNF-α	F	ACTGAACTTCGGGGTGATCG
	R	GCTTGGTGGTTTGCTACGAC
IL-17	F	GTGAAGGCAGCGGTACTCAT
	R	AGGGTGAAGTGGAACGGTTG
IL-23	F	ATAAGCACCTGCTGGACTCG
	R	GGAACGGAGAAGAGAACGCT
IL-10	F	CCAGTCAGCCAGACCCACAT
	R	GCATCACTTCTACCAGGTAAAAC
IL-6	F	AGAGACTTCCAGCCAGTTGC
	R	AGTCTCCTCTCCGGACTTGT
IL-12	F	TGACATGTGGAGCAGCATCT
	R	GGTGGGTCCGGTTTGATGAT
ZO-1	F	GAGTTTGACAGTGGAGTCG
	R	AGCTGAAGGACTCACAGGAA
Muc2	F	GGGGCTATGGCAGACTTTGT
	R	CCCAAGCGAACTCCATTCCT
Occludin	F	TCACTGTGTGACCTGTCTTGG
	R	ACTGGGCTGGATGCCAATTT
TLR4	F	TTCCACAAGAGCCGGAAAGT
	R	GGCGATACAATTCGACCTGC
MyD88	F	TTCTCTCTACCGTTGGTCGC
	R	GCCAGGCATCCAACAAACTG
GADPH	F	GCGAGATCCCGCTAACATCA
	R	CTCGTGGTTCACACCCATCA

Enzyme-Linked Immunosorbent Assay (ELISA)

According to the manufacturer's protocols, the serum was used to detect the expression of TNF-α, IL-1β, IL-6, and IL-10.

Western Blotting Assay

The proteins of colon tissue were extracted by RIPA and isolated using SDS-PAGE. Proteins were then transferred to PVDF membranes following by incubating relevant primary and secondary antibodies. Protein signals were detected with ECL kit on the basis of instructions.

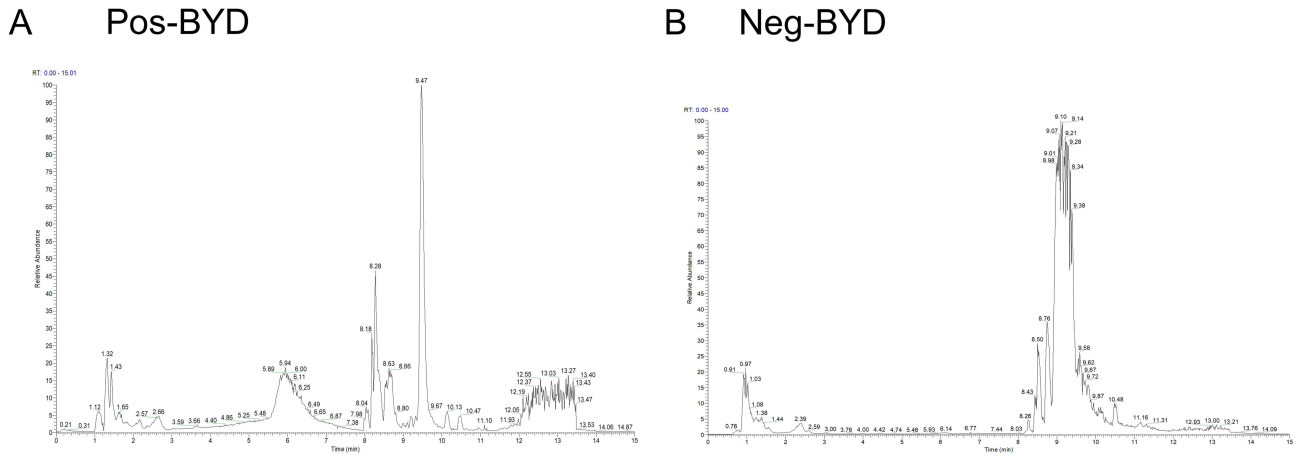

Figure 2 Analysis of the components of BYD by LC-MS/MS. The total ion chromatograms (TIC) of BYD. (**A**) The positive mode and (**B**) the negative mode.

Immunofluorescence

For TLR4, MyD88 and NF-κB (p65) detection, sections were sliced at 3 μm of embedded paraffin. After dewaxing and rehydration, the antigen was blocked with 5% BSA. Then specimens were incubated with primary and secondary antibodies, and finally incubated with DAPI at room temperature for 10 minutes to stain the nuclei.

Statistical Analysis

Using GraphPad Prism software 8 to conduct statistical analysis. Numerical Data are expressed as Mean ± SEM. *T* test was used to compare the mean differences between two groups; one-way ANOVA and Tukey method were used to compare the mean differences between multiple groups. $P < 0.05$ was considered as statistically significant.

Results

Representative Active Constituents in the LC-MS/MS Analysis of BYD

In order to identify the canonical chemical components of BYD, we performed LC-MS/MS and main chemical components were shown in the total ion chromatograms (TIC) by the positive ESI+ (Figure 2A) or negative ESI− mode (Figure 2B). The representative compounds of each herb identified in BYD are listed in Table 4. The extracted ion chromatography (EIC) and chemical structure from PubChem database are shown in Supplementary Figure 1.

Table 4 Chemical Characterization of Bioactive Compounds in BYD

No.	Name	Formula	M/Z	RT (min)	Intensity
①	Berberine	$C_{20}H_{18}NO_4$	336.1213	9.47	285913055232
②	Menisperine	$C_{21}H_{26}NO_4$	356.1834	8.79	4681981440
③	Noroxyhydrastinine	$C_{10}H_9NO_3$	192.0648	9.36	4246476032
④	Gallic acid	$C_7H_6O_5$	171.0279	6.79	495569696
⑤	Catechin	$C_{15}H_{14}O_6$	291.0846	8.41	6343785472
⑥	Ferulic acid	$C_{10}H_{10}O_4$	195.0646	9.32	11300408320
⑦	Indigo	$C_{16}H_{10}N_2O_2$	263.0797	11.74	4425904128
⑧	Uracil	$C_4H_4N_2O_2$	113.0345	4.52	3200797696
⑨	Hypoxanthine	$C_5H_4N_4O$	135.028	0.92	7374364160

Active Ingredients of BYD and "Herb-Compound-Target" Network

In line with OB ≥ 30% and DL ≥ 0.18, 41 bioactive ingredients of BYD were screened using TCMSP database to illustrate the mechanism of BYD (Figure 3A, Supplementary Table 1). Gene names and IDs were obtained from UniProt and matched with BYD active ingredients. We identified 203 compound-related targets after removing duplicates. With "ulcerative colitis" as the key word, disease targets were gained from OMIM, GeneCards, TTD and Drugbank databases, and 1303 disease targets were identified after median screening. Combine 203 active compound-related targets and 1303 UC-related targets, and retain 106 overlapping targets as candidate targets (Figure 3B). To clearly elucidate the relationship between 3 herbs, 41 active ingredients and 203 potential targets in BYD, a 'Herb-Compound-Target' network was constructed, which consists of 246 nodes and 607 edges (Figure 3C). The node with more edges in the network has a higher degree value, and the larger the size of the node, the greater the meaning. The top 3 constituents were quercetin (MOL000098), kaempferol (MOL000422), beta-sitosterol (MOL000358). The data were shown in Table 5. Among them, β-sitosterol is common ingredient of the three herbs and quercetin is one common component of HB and DY.

PPI Network Analysis

The 106 candidate targets were uploaded into STRING 11.5 to build a PPI network, including 106 nodes and 2279 edges (Figure 4A). Nodes represent proteins and edges display protein–protein interactions. For further visualization and analysis, above data were processed by Cytoscape 3.9.1 to construct a novel PPI network, which also included 106 nodes and 2279 edges (Figure 4B). Using the CytoNCA plug-in in Cytoscape, the core targets were mined according to the respective mean values of DC, EC, BC and CC, and then the top 30 were selected to build a network map of core targets with Cytoscape (Figure 4C). As shown in the figure, correlation is proportional to node size and color depth. The top five targets are AKT1, IL-6, TP53, TNF and IL-1β, which can be considered as key targets in the anti-UC pharmacological mechanism of BYD (Table 6).

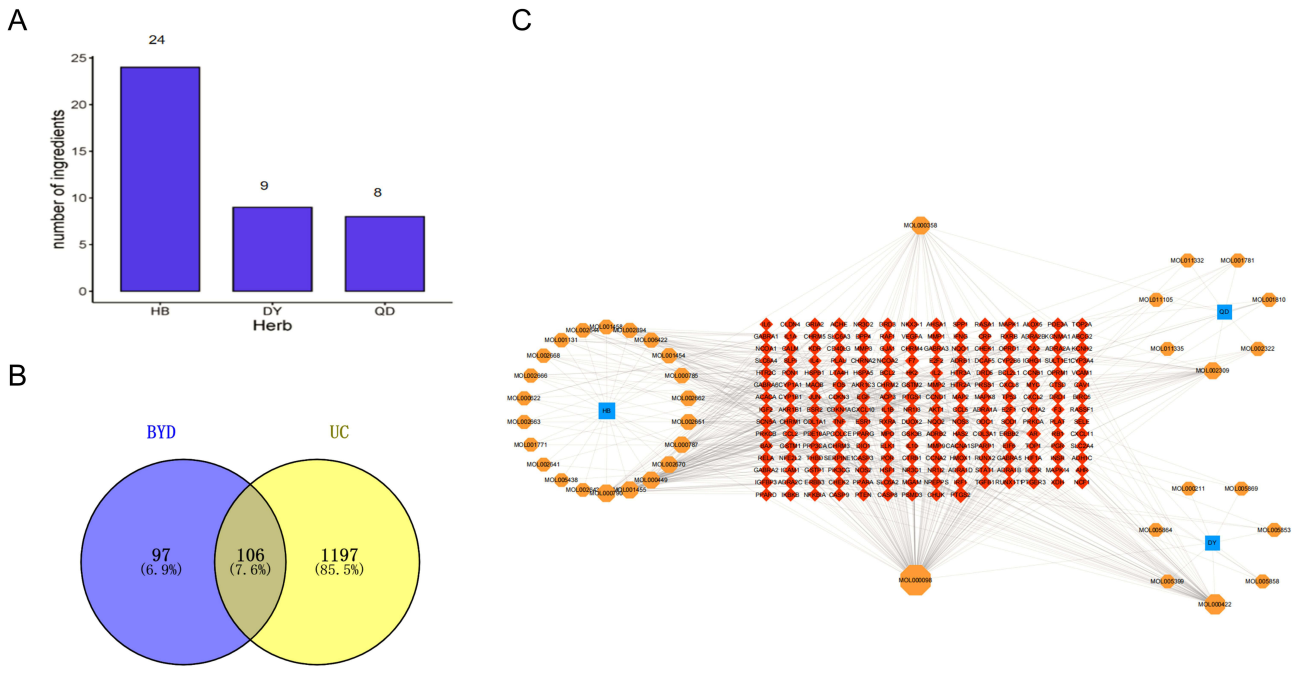

Figure 3 Active Ingredients of BYD and "Herb-Compound-Target" Network. (**A**) The number of ingredients in each herb. (**B**) Distribution Of BYD potential targets and UC targets. (**C**) Herb-Compound-Target network of BYD. Red rhombuses indicate targets. Blue squares represent three herbs: Baiyu, Diyu and Qingdai. Orange octagons show the major components of three herbs, respectively. The color and size of the nodes reflect the degree value. Grey lines indicate the interrelationships between compounds and targets.

Table 5 Top 3 Compounds Information of BYD Network

Mol ID	Molecule Name	Molecule Structure	OB (%)	DL	Degree	Betweenness Centrality	Closeness Centrality
MOL000098	quercetin	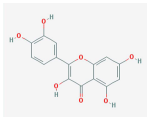	46.43	0.28	144	0.6738	0.5975
MOL000422	kaempferol	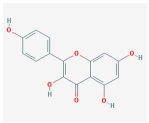	41.88	0.24	57	0.1236	0.4195
MOL000358	beta-sitosterol	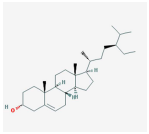	36.91	0.75	37	0.0776	0.3926

GO and KEGG Pathway Enrichment Analysis

In total, 1724 statistically significant GO terms were obtained, incorporating 56 for CC, 1540 for BP and 128 for MF. The top 20 of CC, BP and MF were visualized in a bar graph (Figure 5A). We discovered the significantly GO terms relative to targets of BYD were "response to inorganic substance" (BP), "membrane raft and membrane microdomain" (CC), and "cytokine receptor binding" (MF). The 176 pathways were got by KEGG enrichment analysis, of which the top 30 pathways were exhibited in the form of bubble plots (Figure 5B). Among them, IL-17 signaling pathway (associated with 24 genes), TNF signaling pathway (associated with 25 genes), apoptosis (associated with 20 genes), TOLL-like receptor pathway (associated with 19 genes), NOD-like receptor pathway (associated with 19 genes), NF-κB signaling pathway (associated with 16 genes) are closely related to UC. Finally, we constructed a component-target-pathway network with 277 nodes and 1249 edges to illustrate the potential relationships of herbs, components, targets, and top 30 pathways described above (Figure 5C).

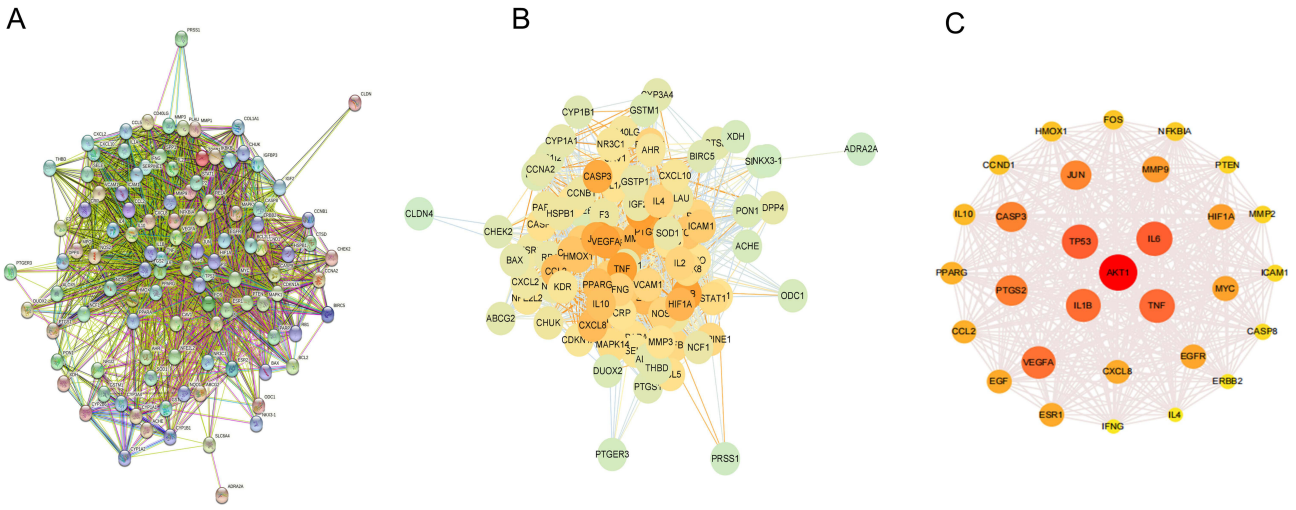

Figure 4 PPI Network Analysis. (**A**) The interactive PPI network obtained from STRING database with the minimum required interaction score set to 0.97. Each node represents relevant targets, and edges stand for protein-protein associations. (**B**) PPI network imported from STRING database to Cytoscape 3.9.1. (**C**) PPI network of more significant proteins extracted from (**B**) by filtering 4 parameters: DC, EC, BC and CC.

Table 6 Top 5 Targets Information of PPI Network

Protein Name	Degree	Betweenness Centrality	Closeness Centrality
AKT1	91	392.4378	0.8750
IL-6	88	413.4313	0.8606
TP53	88	350.4469	0.8536
TNF-α	87	323.555	0.8467
IL-1β	86	354.2278	0.8467

BYD Ameliorates UC Symptoms of Colitis Rat

As clinical practice proves that BYD has ideal therapeutic effect, we tested the efficacy of BYD on UC rats. UC model was established to assess the effects of BYD (Figure 6A). During the experiment, except for the rats in control group, the other rats gradually developed listless, loss of fur gloss, reduction of diet and water intake and even perianal ulceration with the increase of DSS solution drinking time (Figure 6B). After enema administration, above symptoms were relieved. In comparison to model group, the body weight of rats after treatment increased (Figure 6C). DAI score is a vital indicator for assessing UC model. The rats in model group achieved higher scores, enema therapy lowered DAI scores (Figure 6D). In addition, both 5-ASA and BYD could significantly reverse the colon shortening trend (Figure 6E and F). These results demonstrated BYD relieved UC symptoms of colitis rat.

BYD Inhibits the Intestinal Inflammation of Colitis Rat

To illustrate the effect of BYD on intestinal inflammation, we tested the inflammatory factors. The colon tissue structure in control group was intact, and there was no obvious inflammatory cell. But intestinal structural integrity in the model group was destroyed and inflammatory cells can be observed. After the enema with 5-ASA and BYD, the colon tissue morphology could be alleviated, the inflammatory cells were reduced (Figure 6G). The pathological score was statistically significant (Figure 7A). Moreover, we detected the mRNA expression levels of pro-inflammatory factors, such as TNF-α, IL-1β, IL-6, IL-17, IL-23, and IL-12 and anti-inflammatory factor IL-10 (Figure 7B–H). In comparison to control group, TNF-α, IL-1β, IL-6, IL-17, IL-23, and IL-12 increased in model group, while IL-10 decreased. As expected, BYD treatment suppressed pro-inflammatory factors, and upregulated anti-inflammatory factor remarkably. The protein levels of inflammatory factors reflected consistent trend (Figure 7I–L). These data indicated that BYD attenuated colonic inflammation in UC rats.

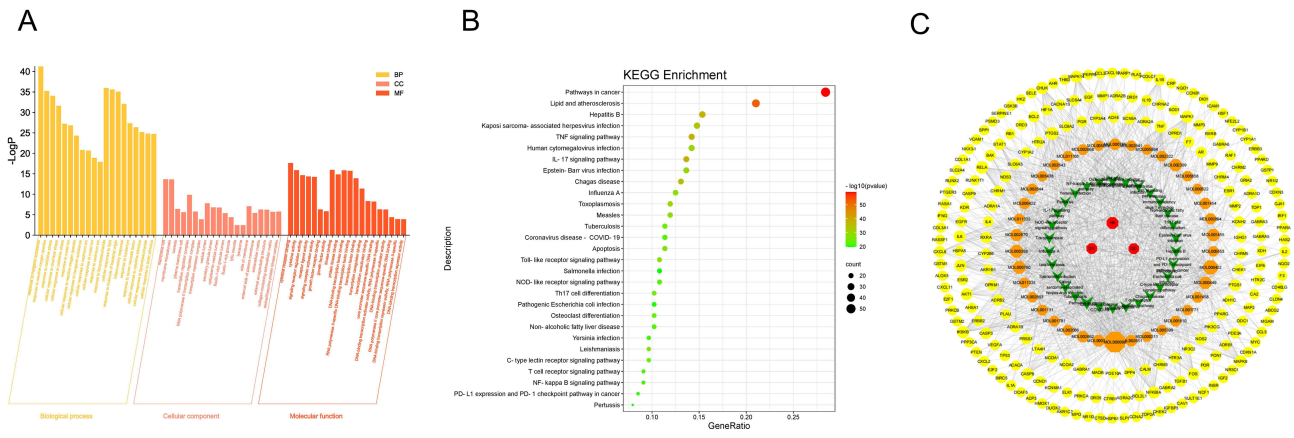

Figure 5 GO and KEGG Pathway Enrichment Analysis. (**A**) GO enrichment analysis for 106 key targets. (**B**) KEGG enrichment analysis for 106 key targets. (**C**) Component-Target-Pathway network. Red octagons indicate three herbs. Orange octagons show ingredients. Yellow circles suggest targets. Green V represent pathways. The color and size of the nodes reflect the degree value. Grey lines indicate the interrelationships between compounds and targets.

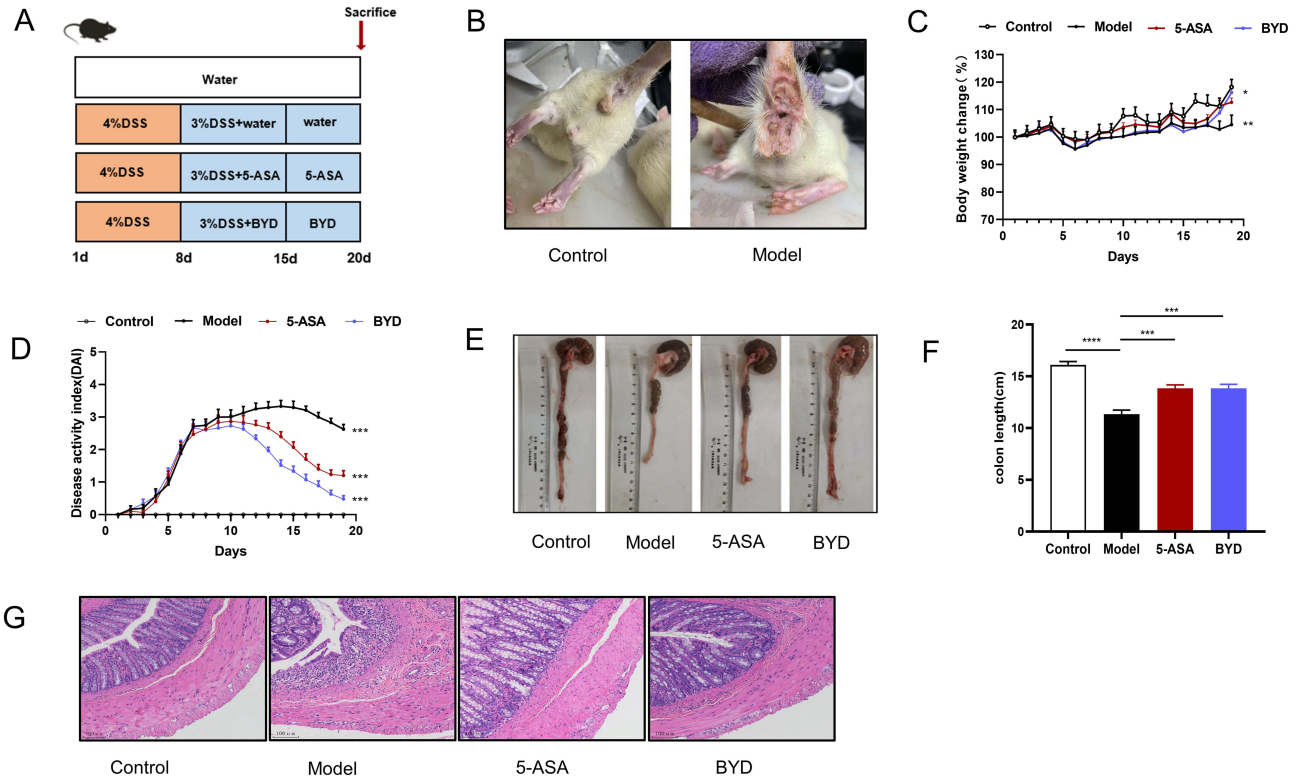

Figure 6 BYD ameliorates UC symptoms of colitis rat. (**A**) Time flow chart. (**B**) Representative images of perianal in control and model group. (**C**) Body weight changes during experiment (n = 6–8). (**D**) Disease active index (DAI) (n = 6–8). (**E**) Representative images of colon (n = 6–8). (**F**) length of colon (n = 6–8). (**G**) Representative H&E-stained colon section (scar bar, 100 μm) (n = 6–8). Data are expressed as Mean ± SEM. * $P < 0.05$, ** $P < 0.01$, *** $P < 0.001$; one-way ANOVA with Tukey's post hoc analysis.

BYD Protects the Intestinal Barrier of Colitis Rat

UC is characterized by abnormal intestinal barrier function, and intestinal barrier biomarkers were detected to demonstrate the protective effects of BYD. As shown, the mucous layer was destroyed and the number of goblet cells was reduced after DSS but reversed after therapy (Figure 8A). The mRNA expression manifested that ZO-1, Muc2 and Occludin in model group were significantly lower than those in control group (Figure 8B–D). Intriguingly, 5-ASA and BYD treatment increased their levels. Furthermore, we evaluated the proteins expression level of ZO-1 and Muc2, reflecting the same tendency (Figure 8E). These data confirmed BYD improved the tight junction structure and promoted the intestinal mucosal barrier repair.

BYD Suppresses TLR4/MyD88/NF-κB Pathway in Colitis Rat

On the basis of network pharmacology data, the TOLL-like receptor pathway, to a large extent, is relevant to the pathogenesis of UC. Thus, we examined the mRNA and protein expression levels of TLR4, MyD88, NF-κB (p65) and P-NF-κB (p-p65). As reported in previous studies, TLR4 and MyD88 were upregulated in the colonic tissues after DSS. These biomarkers were downregulated after BYD treatment (Figure 9A and B). Blue representing the nucleus and red representing p65. The p65 in the control group gathered in the cytoplasm, while p65 in the model group entered the nucleus and was activated. As shown, 5-ASA and BYD could inhibit the activation and phosphorylation of p65 (Figure 9C and D). Combined, BYD might restrain TLR4/MyD88/NF-κB pathway in UC rat.

Molecular Docking Analysis

According to network pharmacology results and animal experiments, quercetin (MOL000098) and kaempferol (MOL000422) were screened for molecular docking with the top 4 targets, AKT1 (PDB ID: 1UNQ), IL-6 (PDB ID: 1ALU), TP53 (PDB ID: 7DHZ) and TLR4 (PDB ID: 2Z62). The binding energy data of molecular docking are displayed in Table 7, manifesting the

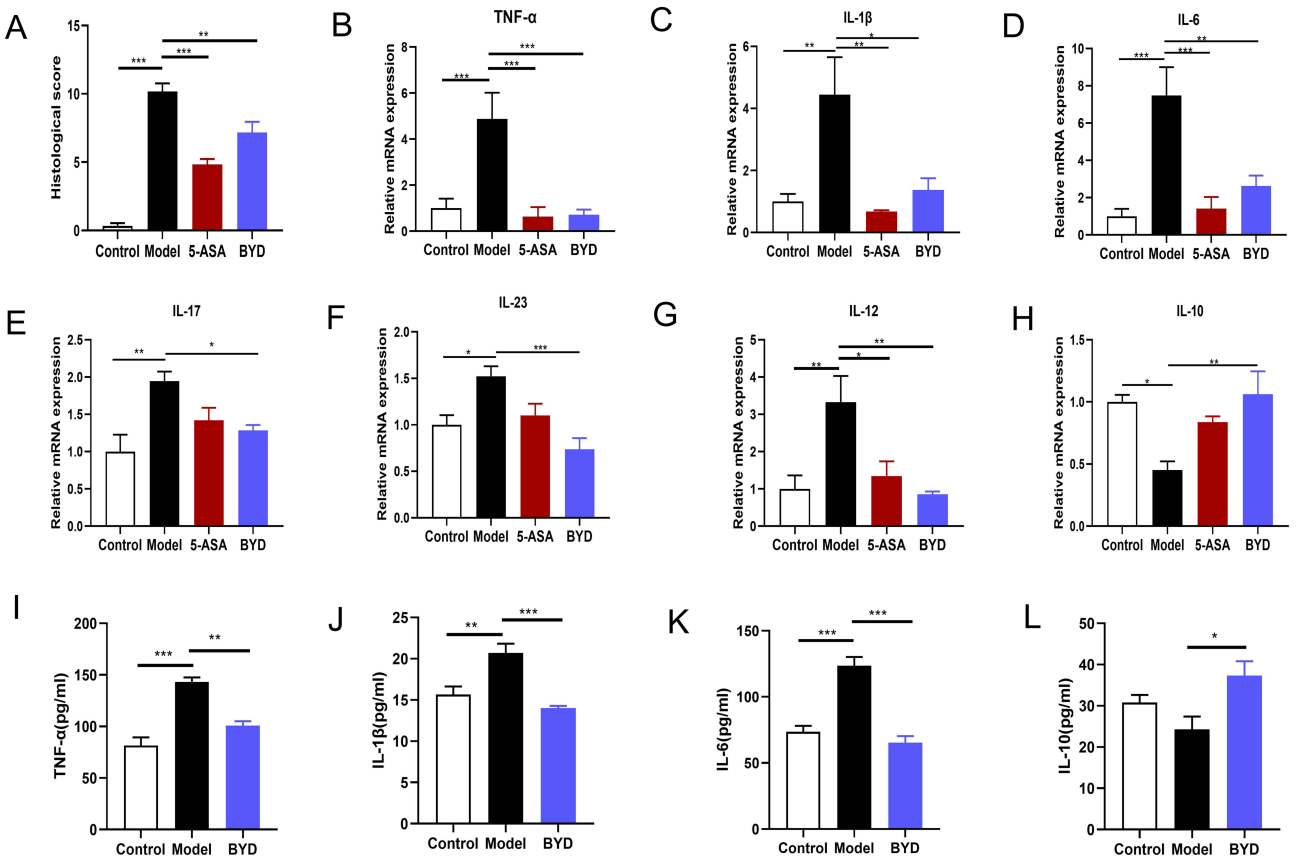

Figure 7 BYD inhibits the intestinal inflammation of colitis rat. (**A**) The histological score (n = 6–8). (**B**–**H**) Relative mRNA expression of TNF-α, IL-1β, IL-6, IL-17, IL-23, IL-12 and IL-10 in the colon tissue of rats (n = 6–8). (**I**–**L**) Relative protein expression of TNF-α, IL-1β, IL-6 and IL-10 in the serum of rats (n = 6–10). Data are expressed as Mean ± SEM. * $P < 0.05$, ** $P < 0.01$, *** $P < 0.001$; one-way ANOVA with Tukey's post hoc analysis.

compound ligand and protein receptor were well docked. Figure 10 shows the local structures of protein receptors and component ligands after visualization via PyMol. Quercetin can interact with GLN-47 through one hydrogen bond, and interact with GLU-40 and LYS-39 through two hydrogen bonds in AKT1 (Figure 10A). Quercetin forms one hydrogen bond with LYS-86, GLU-93 and LEU-64 and two hydrogen bonds with LYS-66 in IL-6 (Figure 10B). Quercetin forms one hydrogen bond with GLU-198, ASN-200 and HIS-233, two hydrogen bonds with THR-231 and four hydrogen bonds with PRO-222 in TP53 (Figure 10C). The structure of quercetin could form one hydrogen bond with PRO-145, PHE-122 and SER-126, and interact with two hydrogen bonds with THR-151 and SER-123 in TLR4 (Figure 10D). Kaempferol interacts with GLN-47 through one hydrogen bond, and interacts with GLU-40 and LYS-39 through two hydrogen bonds in AKT1 (Figure 10E). Kaempferol forms one hydrogen bond with Lys-120, Glu-99, ASN144 and PRO-139 and two hydrogen bonds with GLU-95 in IL-6 (Figure 10F). Kaempferol forms one hydrogen bond with GLU-271, LYS-132, ARG248, ARG174, and SER240 in TP53 (Figure 10G). The structure of kaempferol could form one hydrogen bond with PRO-145, GLY-124, LEU-125, and interact with two hydrogen bonds with PHE-122 and SER-126 in TLR4 (Figure 10H).

Discussion

Patients suffering from UC, a progressive disease, often face the risks of intestinal motility disorders, anorectal dysfunction and colorectal cancer, and even colectomy is required in severe cases.[2] Therefore, it is imperative to clarify the pathogenesis of UC and develop creative drugs.

In this study, the conceivable mechanism of BYD against UC was revealed using comprehensive network pharmacology and further verified by animal experiment and molecular docking. We identified 41 active compounds in BYD, 203 targets associated with compounds and 1303 UC-related targets from various databases. After matching, 106 targets

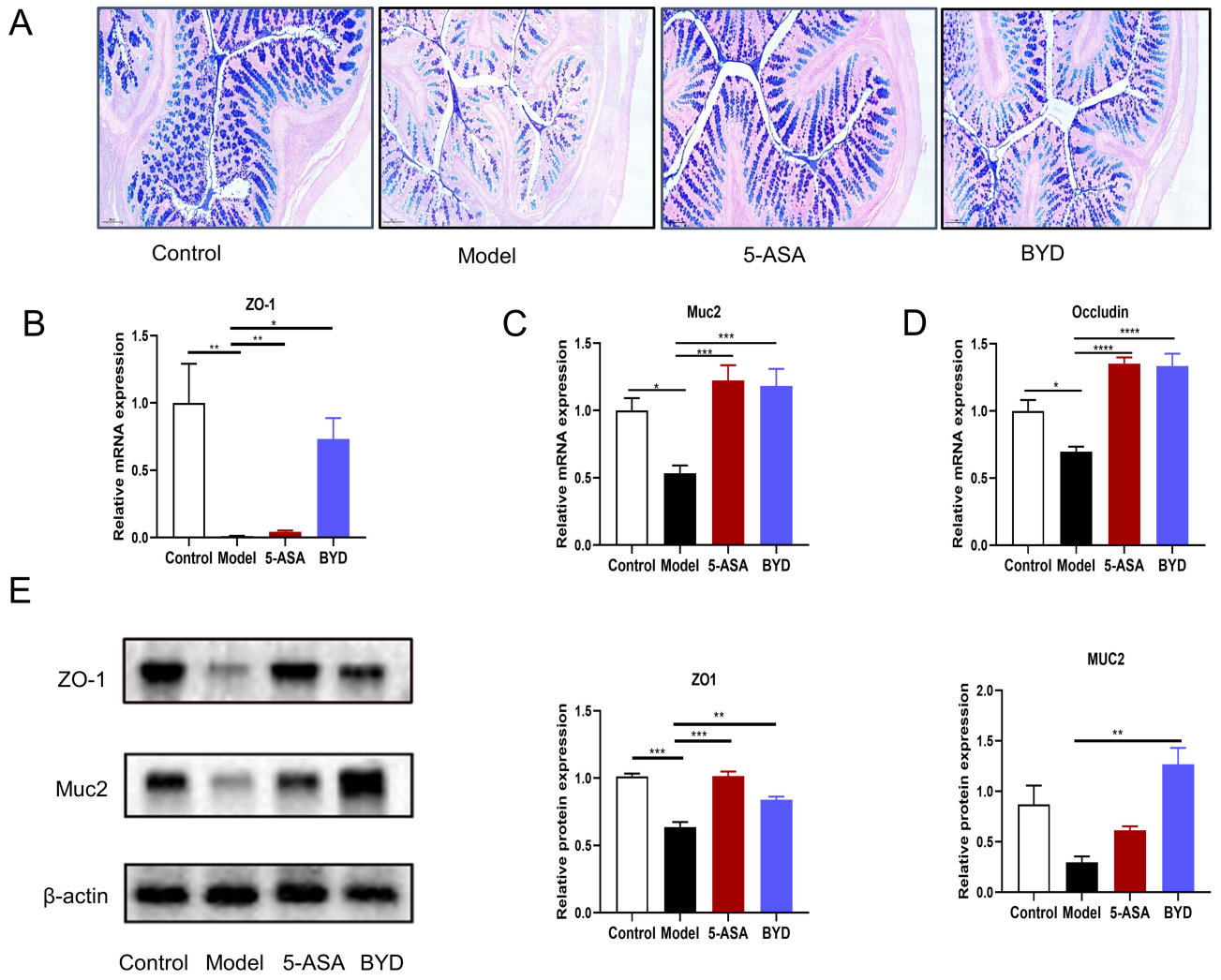

Figure 8 BYD protects the intestinal barrier of colitis rat. (**A**) Representative AB/PAS-stained colonic tissue section (scar bar, 100 μm). (**B**–**D**) Relative mRNA expression of ZO-1, Muc2, Occludin in the colon tissue of rats (n = 6–8). (**E**) Immunoblots of ZO-1 and Muc2 in the colon tissue of Rats. Data are expressed as Mean ± SEM. * $P < 0.05$, ** $P < 0.01$, *** $P < 0.001$, **** $P < 0.0001$; one-way ANOVA with Tukey's post hoc analysis.

were associated with both compounds and UC. The main components, quercetin, kaempferol and beta-sitosterol, and the pivotal targets, AKT1, IL-6, TP53, TNF and IL-1β, may explain the anti-UC effect of BYD.

Quercetin can influence the expression of pro-inflammatory cytokines, injury repair molecules and NF-κB inhibitory molecules, which demonstrates advantageous influences on primary pathways involved in DSS-induced UC.[27] An organoid experiment related to ulcerative colitis confirmed the positive effect of quercetin on colitis.[28] Another study has shown that quercetin reduces colonic injury, regulates MPO activity and MDA levels, and significantly increases glutathione (GSH) content in TNBS-induced mouse colitis models.[29] An experiment in vitro and in vivo showed that beta-sitosterol can reduce the levels of inflammatory cytokines in the colon tissues of mice with colitis, and the expression of antimicrobial peptides was increased and the survival rate of Salmonella typhimurium was decreased in beta-sitosterol-treated intestinal epithelial cells.[30] Kaempferol ameliorated colitis in mice mainly through phenylalanine metabolism, galactose metabolism, arginine and proline metabolism.[31] Current studies have demonstrated that UC is driven by type 2 helper T cells (Th2), and several proinflammatory immune cytokines derived from the lamina propria play a key role in the pathogenesis of UC.[32] Increased intestinal levels of the inflammatory cytokines including TNF-α, IL-6 and IL-1β are positively associated with disease activity and severity. TNF-α secreted by monocytes, macrophages and natural killer cells can significantly destroy intestinal barrier resistance, and lead to barrier defects unique to UC.[33] The ideal therapeutic effects of anti-TNF-α therapy include a sustained anti-inflammatory response, mucosal healing and

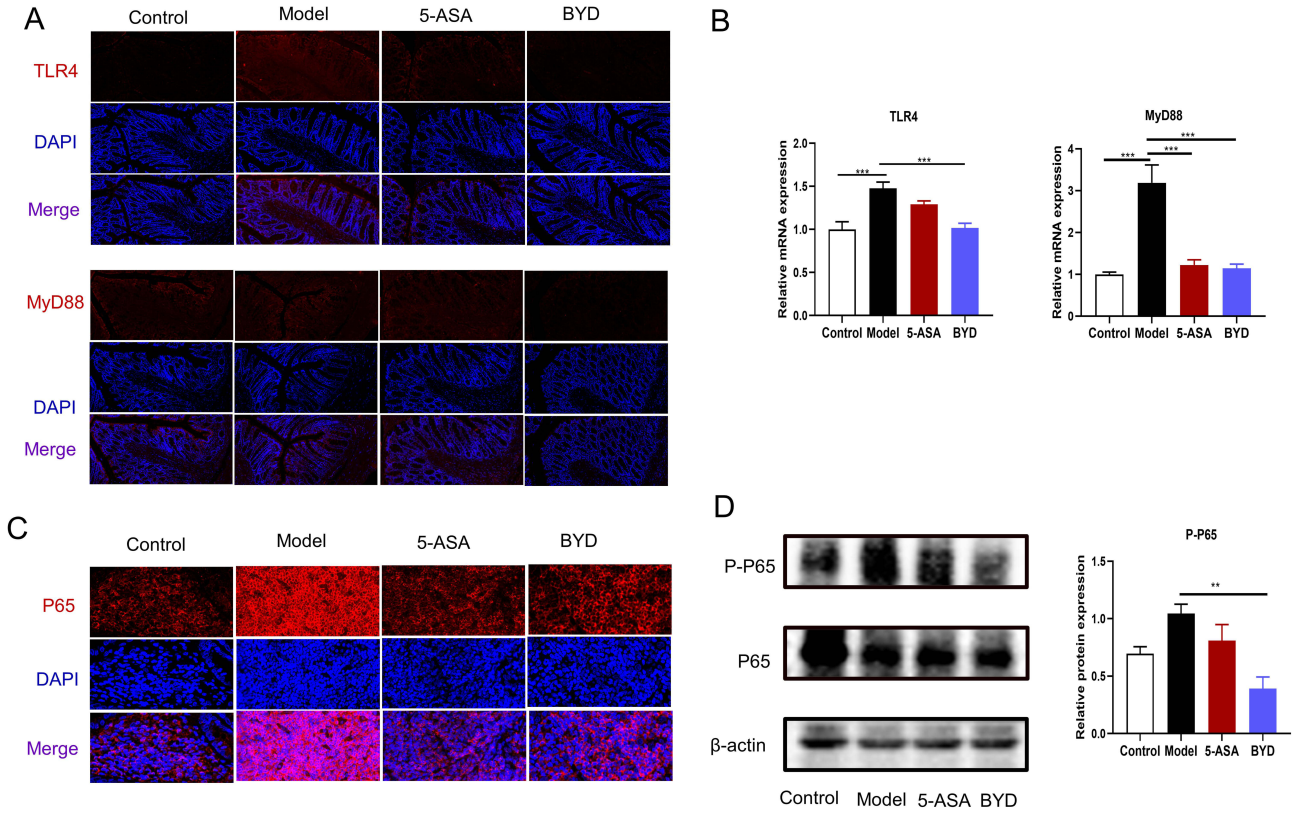

Figure 9 BYD suppresses TLR4/MyD88/NF-κB signaling pathway in colitis rat. (**A**) Immunofluorescence of TLR4, MyD88. (**B**) Relative mRNA expression of TLR4 and MyD88 in the colon tissue of rats (n = 6–8). (**C**) Immunofluorescence of p65. (**D**) Immunoblots of p65 and p-p65 in the colon tissue of rats. Data are expressed as Mean ± SEM. ** $P < 0.01$, *** $P < 0.001$; one-way ANOVA with Tukey's post hoc analysis.

restoration of the gut epithelial barrier function. One research showed that anti-TNF-α therapy reduced histological and endoscopic disease activity, inhibited immune cell activation, downregulated expression of cell adhesion molecules and proinflammatory cytokines, regulated apoptosis of monocytes and enterocytes, and restored gut barrier function

Table 7 The Binding Energy of Compound and Core Targets (Kcal/Mol)

Target	PDB ID	Target Structure	Compound	Affinity (kcal/mol)
AKT1	1UNQ	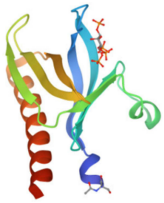	Quercetin	−5.92
			kaempferol	−6.34
IL-6	1ALU	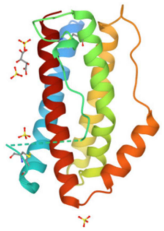	Quercetin	−5.76
			kaempferol	−6.14

(*Continued*)

Table 7 (Continued).

Target	PDB ID	Target Structure	Compound	Affinity (kcal/mol)
TP53	7DHZ		Quercetin	−6.47
			kaempferol	−7.26
TLR4	2Z62	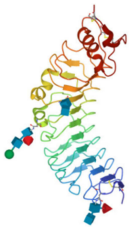	Quercetin	−6.83
			kaempferol	−6.31

and antimicrobial peptide levels.[34] IL-1β, a multifunctional cytokine, can induce targets such as IL-6, IL-8, and COX2, stimulate T cell proliferation, and direct neutrophils to the infection site. IL-6 can mediate the immune response by recruiting monocytes and lymphocytes to replace neutrophils in shifting from innate immunity to adaptive immunity.[35] More and more studies have shown that TP53, a tumor suppressor gene, is the most frequently mutated gene in IBD-related dysplastic lesions and cancers.[36] Similarly, noncoding TP53 mutations are enriched in IBD–associated colorectal cancers.[37] These suggest that BYD may inhibit colorectal cancer associated with colitis. AKT signaling pathway mainly is associated with cell proliferation.[38] The results above manifest that BYD characteristically is multi-component and multi-target drugs with synergistic effects.

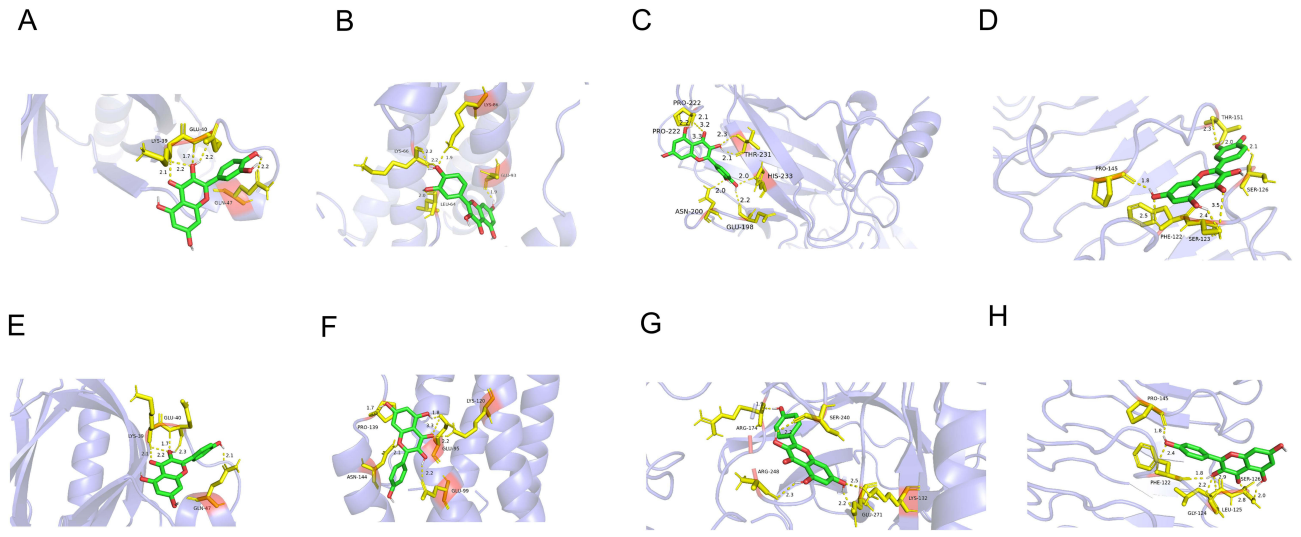

Figure 10 Molecular Docking Analysis. (**A**) AKT1 with quercetin; (**B**) IL-6 with quercetin; (**C**) TP53 with quercetin. (**D**) TLR4 with quercetin. (**E**) AKT1 with kaempferol. (**F**) IL-6 with kaempferol. (**G**) TP53 with kaempferol. (**H**) TLR4 with kaempferol. The hydrogen bonds were indicated by dashed lines and the length was added around the lines.

For further exploration of the mechanism of BYD, GO and KEGG analyses were performed. GO results were principally related to biological processes, such as inflammatory response, immune regulation, signal transduction, and apoptosis. KEGG enriched 176 pathways, among which TNF signaling pathway, IL-17 signaling pathway, apoptosis, TOLL-like receptor pathway, NOD-like receptor pathway and NF-κB signaling pathway were related to UC, indicating the therapeutic effect of BYD on UC through multiple pathways. TOLL-like receptor is one of the pattern recognition receptors that mediate innate immune responses.[39] Except for TLR3, other activated TLRs mainly signal through MyD88, ultimately activating NF-κB and MAPK (Figure 11).[40] TLR4, the first TLR identified in mammals, recognizes LPS in Gram-negative bacteria. Under physiologic conditions, TLR4 is expressed at a low level in IECs.[41] Study shows that TLR4 and NF-κB expression are positively correlated with disease in Chinese UC patients.[40]

Network pharmacological results were further validated by animal experiments. These results manifested that BYD could reduce body weight loss, improve DAI score and reverse colon shortening in colitis rats. As mentioned in the above section, BYD did downregulate the expression of inflammatory factors, while increasing the expression of anti-inflammatory factor in UC rats. UC is considered as an aberrant intestinal barrier disease. The intestinal epithelium is the gateway between the host immune response and the gut microbiota. Thus, therapeutic goal has evolved from symptom relief to mucosal healing.[42,43] We detected biomarkers of the intestinal barrier, suggesting that BYD could protect the intestinal mucosa. Besides, we demonstrated that BYD could dramatically inhibit TLR4/MyD88/NF-κB pathway. Finally, we screened two core biologically active compounds, quercetin, kaempferol, and four representative targets, IL-6, TP53, AKT1, TLR4. The molecular docking results show that these compounds can bind to the proteins very well, indicating that the combination is stable.

The limitation of this study is that only ingredients screened through the database, without combining the components measured by LC-MS/MS analysis, were subjected to network pharmacological analysis. At present, a large number of studies have taken oral administration as the main strategy for the treatment of UC, and there are few researches on rectal administration for UC. Compared to the many systemic adverse reactions associated with oral administration, enema treatment can reduce these adverse reactions. It is worth noting that the enema method can make the drug directly act on the intestinal lesion site, quickly reduce local inflammation, promote ulcer healing, and repair damaged intestinal tissue. Although animal studies on oral treatment of UC by HB, DY and QD have been published, no studies on the treatment of UC by rectal administration of these

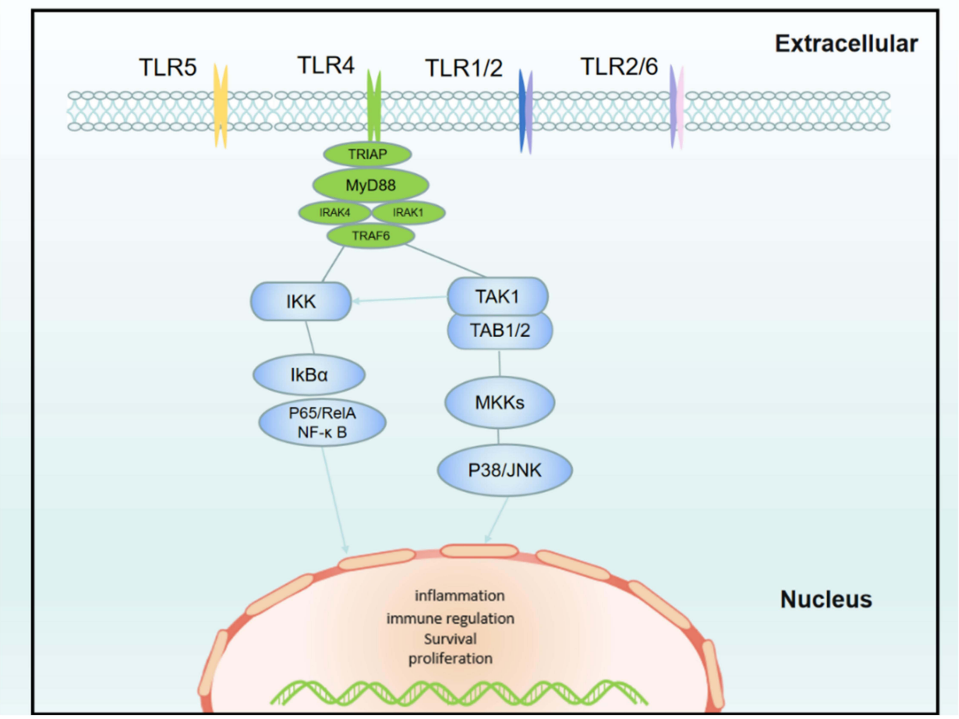

Figure 11 TOLL-like receptor signaling pathway.

three traditional Chinese medicines have been reported. Our study demonstrated that BYD has favorable effects in the treatment of UC by enema. Surprisingly, during the treatment of UC rats by enema, we found that the perianal ulceration of the rats in BYD group was relieved faster and to a lesser extent than that in 5-ASA group when the drug solution was infiltrated into the anus of the rats. Thus, despite its limitations, in addition to its desirable efficacy, another advantage of BYD is that its safety can be widely accepted by patients.

Conclusion

In this study, we used a comprehensive strategy combining network pharmacological analysis, molecular docking analysis and animal experimental validation to reveal the potential pharmacological mechanism of BYD for the treatment of UC, and determine the involved effective active component, core genes and possible signaling pathways. Animal experiment verified that BYD improved DAI score and histopathological damage, down-regulated inflammatory factor levels, repaired the intestinal barrier, and inhibited the TOLL-like receptor pathway in UC rats. The main active ingredients of BYD (quercetin, kaempferol) showed good stability with the targets (IL-6, TP53, AKT1 and TLR4). Our study reveals that BYD is beneficial for improving UC and provides a theoretical basis for the development of enema drugs for the treatment of UC. As an autoimmune disorder with lesions in the intestinal tract, UC can be managed by a combination of oral and rectal administration in clinical practice, which encourages researchers to focus not only on oral medications, but also on the rectal administration of medications for the treatment of UC in the future.

Abbreviations

5-ASA, 5-aminosalicylic acid; BP, biological process; BYD, Baiyu decoction; CC, cellular component; EIC, extracted ion chromatography; DAI, disease activity index; DL, Drug-likeness; DSS, dextran sodium sulfate; DY, Diyu; GO, Gene Ontology; HB, Huangbai; IBD, Inflammatory bowel disease; KEGG, Kyoto Encyclopedia of Genes and Genomes; LC-MS/MS, liquid chromatography-mass spectrometry; MF, molecular function; MyD88, myeloid differentiation factor 88; OB, Oral bioavailability; PPI, protein–protein interaction; QD, Qingdai; TCM, Traditional Chinese medicine; TCMSP, Traditional Chinese Medicine Systems Pharmacology Database and Analysis Platform; TLR4, TOLL-like receptor 4; UC, Ulcerative colitis.

Ethics Statement

All databases in this study are public databases, the contents of which are publicly available and allow unrestricted reuse through open licenses. According to official document issued by National Science and Technology Ethics Committee of China, the use of legally obtained public data is not subject to ethical scrutiny (https://www.gov.cn/zhengce/zhengceku/2023-02/28/content_5743658.htm). Therefore, the part of this study involving public databases would have the need for ethics approval waived (Ethics Committee in Affiliated Hospital of Nanjing University of Traditional Chinese Medicine). The animal studies were approved by the Animal Ethics Committee in Affiliated Hospital of Nanjing University of Traditional Chinese Medicine (Application Number: 2023DW-030-01) in accordance with the guidelines of the Guide for the Care and Use of Laboratory Animals.

Acknowledgments

This work was supported by Jiangsu Administration of Traditional Chinese Medicine (No. K2021J20), National Administration of Traditional Chinese Medicine High-level Key Discipline Project of Traditional Chinese Medicine (National TCM Human Education Letter (2023) No. 85)and Jiangsu Province Traditional Chinese Medicine Digestive Disease Medical Innovation Center (Su Health Science and Education (2022) No. 15).

Author Contributions

All authors made a significant contribution to the work reported, whether that is in the conception, study design, execution, acquisition of data, analysis and interpretation, or in all these areas; took part in drafting, revising or critically reviewing the article; gave final approval of the version to be published; have agreed on the journal to which the article

has been submitted; and agree to be accountable for all aspects of the work. Hong Shen is the first corresponding author and Lei Zhu is the second corresponding author.

Disclosure

The authors report no conflicts of interest in this work.

References

1. Hibi T, Ogata H. Novel pathophysiological concepts of inflammatory bowel disease. *J Gastroenterol*. 2006;41(1):10–16. doi:10.1007/s00535-005-1744-3
2. Kobayashi T, Siegmund B, Le Berre C, et al. Ulcerative colitis. *Nat Rev Dis Primers*. 2020;6(1):74. doi:10.1038/s41572-020-0205-x
3. Ungaro R, Mehandru S, Allen PB, Peyrin-Biroulet L, Colombel JF. Ulcerative colitis. *Lancet*. 2017;389(10080):1756–1770. doi:10.1016/s0140-6736(16)32126-2
4. Matsuoka K, Kobayashi T, Ueno F, et al. Evidence-based clinical practice guidelines for inflammatory bowel disease. *J Gastroenterol*. 2018;53(3):305–353. doi:10.1007/s00535-018-1439-1
5. Harbord M, Eliakim R, Bettenworth D, et al. Third European evidence-based consensus on diagnosis and management of ulcerative colitis. part 2: current management. *J Crohns Colitis*. 2017;11(7):769–784. doi:10.1093/ecco-jcc/jjx009
6. Hopkins AL. Network pharmacology: the next paradigm in drug discovery. *Nat Chem Biol*. 2008;4(11):682–690. doi:10.1038/nchembio.118
7. Fotis C, Antoranz A, Hatziavramidis D, Sakellaropoulos T, Alexopoulos LG. Network-based technologies for early drug discovery. *Drug Discov Today*. 2018;23(3):626–635. doi:10.1016/j.drudis.2017.12.001
8. Li S, Zhang B. Traditional Chinese medicine network pharmacology: theory, methodology and application. *Chin J Nat Med*. 2013;11(2):110–120. doi:10.1016/s1875-5364(13)60037-0
9. Luo TT, Lu Y, Yan SK, Xiao X, Rong XL, Guo J. Network pharmacology in research of Chinese medicine formula: methodology, application and prospective. *Chin J Integr Med*. 2020;26(1):72–80. doi:10.1007/s11655-019-3064-0
10. Villoutreix BO, Bastard K, Sperandio O, et al. In silico-in vitro screening of protein-protein interactions: towards the next generation of therapeutics. *Curr Pharm Biotechnol*. 2008;9(2):103–122. doi:10.2174/138920108783955218
11. Vakser IA. Protein-protein docking: from interaction to interactome. *Biophys J*. 2014;107(8):1785–1793. doi:10.1016/j.bpj.2014.08.033
12. Sun Y, Lenon GB, Yang AWH. Phellodendri cortex: a phytochemical, pharmacological, and pharmacokinetic review. *Rev Evid-Based Complement Altern Med*. 2019;2019:45. 7621929. doi:10.1155/2019/7621929
13. Su S, Wang X, Xi X, et al. Phellodendrine promotes autophagy by regulating the AMPK/mTOR pathway and treats ulcerative colitis. *J Cell Mol Med*. 2021;25(12):5707–5720. doi:10.1111/jcmm.16587
14. Zhou P, Li J, Chen Q, et al. A comprehensive review of genus sanguisorba: traditional uses, chemical constituents and medical applications. *Front Pharmacol*. 2021;12:750165. doi:10.3389/fphar.2021.750165
15. Yasueda A, Kayama H, Murohashi M, et al. Sanguisorba officinalis L. derived from herbal medicine prevents intestinal inflammation by inducing autophagy in macrophages. *Sci Rep*. 2020;10(1):9972. doi:10.1038/s41598-020-65306-4
16. Yu H, Li TN, Ran Q, Huang QW, Wang J. Strobilanthes cusia (Nees) Kuntze, a multifunctional traditional Chinese medicinal plant, and its herbal medicines: a comprehensive review. *J Ethnopharmacol*. 2021;265:113325. doi:10.1016/j.jep.2020.113325
17. Ben-Horin S, Salomon N, Karampekos G, et al. Curcumin-qingdai combination for patients with active ulcerative colitis: a randomized, double-blinded, placebo-controlled trial. *Clin Gastroenterol Hepatol*. 2023. doi:10.1016/j.cgh.2023.05.023
18. Yang QY, Ma LL, Zhang C, et al. Exploring the mechanism of indigo naturalis in the treatment of ulcerative colitis based on TLR4/MyD88/NF-κB signaling pathway and gut microbiota. *Front Pharmacol*. 2021;12:674416. doi:10.3389/fphar.2021.674416
19. Ru J, Li P, Wang J, et al. TCMSP: a database of systems pharmacology for drug discovery from herbal medicines. *J Cheminform*. 2014;6(1):13. doi:10.1186/1758-2946-6-13
20. Ding P, Liu J, Li Q, et al. Investigation of the active ingredients and mechanism of hudi enteric-coated capsules in DSS-induced ulcerative colitis mice based on network pharmacology and experimental verification. *Drug Des Devel Ther*. 2021;15:4259–4273. doi:10.2147/dddt.S326029
21. Amberger JS, Bocchini CA, Schiettecatte F, Scott AF, Hamosh A. OMIM.org: online Mendelian Inheritance in Man (OMIM®), an online catalog of human genes and genetic disorders. *Nucleic Acids Res*. 2015;43(Database issue):D789–98. doi:10.1093/nar/gku1205
22. Szklarczyk D, Gable AL, Lyon D, et al. STRING v11: protein-protein association networks with increased coverage, supporting functional discovery in genome-wide experimental datasets. *Nucleic Acids Res*. 2019;47(D1):D607–d613. doi:10.1093/nar/gky1131
23. Li X, Wei S, Niu S, et al. Network pharmacology prediction and molecular docking-based strategy to explore the potential mechanism of huanglian jiedu decoction against sepsis. *Comput Biol Med*. 2022;144:105389. doi:10.1016/j.compbiomed.2022.105389
24. Ma X, Hu Y, Li X, et al. Periplaneta americana ameliorates dextran sulfate sodium-induced ulcerative colitis in rats by keap1/nrf-2 activation, intestinal barrier function, and gut microbiota regulation. *Front Pharmacol*. 2018;9:944. doi:10.3389/fphar.2018.00944
25. Li Q, Cui Y, Xu B, et al. Main active components of Jiawei Gegen Qinlian decoction protects against ulcerative colitis under different dietary environments in a gut microbiota-dependent manner. *Pharmacol Res*. 2021;170:105694. doi:10.1016/j.phrs.2021.105694
26. Ke H, Li F, Deng W, et al. Metformin exerts anti-inflammatory and mucus barrier protective effects by enriching akkermansia muciniphila in mice with ulcerative colitis. *Front Pharmacol*. 2021;12:726707. doi:10.3389/fphar.2021.726707
27. Maslin LA, Weeks BR, Carroll RJ, Byrne DH, Turner ND. Chlorogenic acid and quercetin in a diet with fermentable fiber influence multiple processes involved in DSS-induced ulcerative colitis but do not reduce injury. *Nutr*. 2022;14(18):3706. doi:10.3390/nu14183706
28. Dicarlo M, Teti G, Verna G, et al. Quercetin exposure suppresses the inflammatory pathway in intestinal organoids from winnie mice. *Int J Mol Sci*. 2019;20(22):5771. doi:10.3390/ijms20225771
29. Dodda D, Chhajed R, Mishra J, Padhy M. Targeting oxidative stress attenuates trinitrobenzene sulphonic acid induced inflammatory bowel disease like symptoms in rats: role of quercetin. *Indian J Pharmacol*. 2014;46(3):286–291. doi:10.4103/0253-7613.132160

30. Ding K, Tan YY, Ding Y, et al. β-Sitosterol improves experimental colitis in mice with a target against pathogenic bacteria. *J Cell Biochem*. 2019;120(4):5687–5694. doi:10.1002/jcb.27853
31. Qu Y, Li X, Xu F, et al. Kaempferol alleviates murine experimental colitis by restoring gut microbiota and inhibiting the LPS-TLR4-NF-κB Axis. *Front Immunol*. 2021;12:679897. doi:10.3389/fimmu.2021.679897
32. Camoglio L, Te Velde AA, Tigges AJ, Das PK, Van Deventer SJ. Altered expression of interferon-gamma and interleukin-4 in inflammatory bowel disease. *Inflamm Bowel Dis*. 1998;4(4):285–290. doi:10.1002/ibd.3780040406
33. Lissner D, Schumann M, Batra A, et al. Monocyte and m1 macrophage-induced barrier defect contributes to chronic intestinal inflammation in IBD. *Inflamm Bowel Dis*. 2015;21(6):1297–1305. doi:10.1097/mib.0000000000000384
34. Gareb B, Otten AT, Frijlink HW, Dijkstra G, Kosterink JGW. Review: local Tumor necrosis factor-α inhibition in inflammatory bowel disease. *Pharmaceutics*. 2020;12(6):539. doi:10.3390/pharmaceutics12060539
35. Ranson N, Kunde D, Eri R. Regulation and sensing of inflammasomes and their impact on intestinal health. *Int J Mol Sci*. 2017;18(11):2379. doi:10.3390/ijms18112379
36. Wanders LK, Cordes M, Voorham Q, et al. IBD-associated dysplastic lesions show more chromosomal Instability than sporadic adenomas. *Inflamm Bowel Dis*. 2020;26(2):167–180. doi:10.1093/ibd/izz171
37. Rajamäki K, Taira A, Katainen R, et al. Genetic and epigenetic characteristics of inflammatory bowel disease-associated colorectal cancer. *Gastroenterol*. 2021;161(2):592–607. doi:10.1053/j.gastro.2021.04.042
38. Adlung L, Kar S, Wagner MC, et al. Protein abundance of AKT and ERK pathway components governs cell type-specific regulation of proliferation. *Mol Syst Biol*. 2017;13(1):904. doi:10.15252/msb.20167258
39. Kordjazy N, Haj-Mirzaian A, Haj-Mirzaian A, et al. Role of toll-like receptors in inflammatory bowel disease. *Pharmacol Res*. 2018;129:204–215. doi:10.1016/j.phrs.2017.11.017
40. Lu Y, Li X, Liu S, Zhang Y, Zhang D. Toll-like receptors and inflammatory bowel disease. *Front Immunol*. 2018;9:72. doi:10.3389/fimmu.2018.00072
41. Toiyama Y, Araki T, Yoshiyama S, Hiro J, Miki C, Kusunoki M. The expression patterns of Toll-like receptors in the ileal pouch mucosa of postoperative ulcerative colitis patients. *Surg Today*. 2006;36(3):287–290. doi:10.1007/s00595-005-3144-y
42. Ungaro R, Colombel JF, Lissoos T, Peyrin-Biroulet L. A treat-to-target update in ulcerative colitis: a systematic review. *Am J Gastroenterol*. 2019;114(6):874–883. doi:10.14309/ajg.0000000000000183
43. Colombel JF, D'Haens G, Lee WJ, Petersson J, Panaccione R. Outcomes and strategies to support a treat-to-target approach in inflammatory bowel disease: a systematic review. *J Crohns Colitis*. 2020;14(2):254–266. doi:10.1093/ecco-jcc/jjz131